JOINT EUROPEAN TORUS

JET–P(93)72

R. Myrnäs, C. Jupén, G. Miecznick,
I. Martinson, B. Denne-Hinnov

Transitions in Boronlike Ni XXIV, Kr XXXII and Mo XXXVIII and Fluorinelike Zr XXXII and Mo XXXIV, observed in the JET Tokamak

Transitions in Boronlike Ni XXIV, Kr XXXII and Mo XXXVIII and Fluorinelike Zr XXXII and Mo XXXIV, observed in the JET Tokamak

R. Myrnäs[1], C. Jupén[1], G. Miecznick[1],
I. Martinson[1], B. Denne-Hinnov

JET-Joint Undertaking, Culham Science Centre, OX14 3DB, Abingdon, UK

[1]Department of Physics, University of Lund, Lund, Sweden.

Preprint of a paper to be published in
Physica Scripta
September 1993

ABSTRACT

Spectra of highly ionized Ni, Ge, Kr, Zr and Mo obtained from the JET tokamak have been studied. In total 20 new lines have been classified as n = 2, $\Delta n = 0$ transitions in B-like and F-like ions. Among the identified lines are M1 transitions within the $2s^22p^5\ ^2P$ ground term of F-like Zr and Mo and within the $2s^22p\ ^2P$ ground term of B-like Mo. Furthermore, for B-like Ni, Kr and Mo, the $2s2p^2\ ^4P_{1/2}$ and $^4P_{5/2}$ levels, which decay by spin-forbidden transitions, have been found. From the observed wavelengths 20 new energy levels were determined. The experiments have been complemented with multiconfiguration Dirac-Fock (MCDF) calculations and semiempirical analyses of transition energies in the B I and F I isoelectronic sequences.

1. INTRODUCTION

The structure of multiply charged ions with 3 - 9 electrons (Li I - F I isoelectronic sequences) is of considerable interest to basic atomic theory, because of the presence of fundamental effects such as electron correlation, relativity and quantum electrodynamics (QED). Transitions in these ions, in particular the n = 2, $\Delta n = 0$ combinations, are of vital importance in the diagnostics of astrophysical and laboratory plasmas. While astrophysical data are not available for elements heavier that Ni (Z = 28), several laboratory light sources for highly charged ions, e.g. laser-produced plasmas, tokamak discharges and fast excited ions, permit extensions of the work to much higher values of Z. For instance, recent studies at the JET tokamak have provided new data for the n = 2 levels from Li-like to F-like Kr [1] and Li-like and Be-like Mo [2]. In the present work we report new analyses of spectra from the JET facility, the emphasis now being placed on highly charged B-like ions of Ni, Ge, Kr and Mo. Some limited studies of F-like Zr and Mo are also reported.

About 10 years ago, Edlén [3, 4] reported systematic studies of the structure of the n = 2, $\Delta n = 0$ transitions for Li-like to F-like ions. The work included detailed comparisons of experimental results and the theoretical data of Cheng et al. [5] who employed the relativistic multiconfiguration Dirac-Fock (MCDF) formalism. For all transitions studied, Edlén derived Z-dependent functions to represent the relatively small differences between experimental and theoretical energies. From these functions recommended values for transition wavelengths were obtained.

Edlén's analyses of B-like [3] and F-like [4] ions are particularly relevant for the present work.

In 1983 virtually no experimental results for B-like ions beyond Ni XXIV were available [3], whereas F-like ions up to Y XXX had already been studied [4]. In the following years additional data have appeared for B-like Zn, Ge and Se [6, 7], Br [8] and Kr [1]. Except for the Br-experiment, which was based on observations of laser-produced plasmas, the other new results were obtained at tokamaks. Of these, Refs. [7] and [1] also provide data for F-like ions. A number of additional studies, using laser-produced plasmas, have also been reported [9-11] for these ions. It is worth noting that Edlén's studies [3, 4] revealed that some of the experimental material for highly charged Ni had comparatively large uncertainties. However, new and much more accurate data for Ni ions have now been reported by Sugar et al. [12] who observed tokamak plasmas.

The present investigation deals with spectra containing transitions in B-like Ni XXIV, Ge XXVIII, Kr XXXII and Mo XXXVIII and F-like Zr XXXII and Mo XXXIV, recorded on the JET tokamak. To aid in the analyses of the observed data we have also performed MCDF calculations, using the code by Grant et al. [13, 14].

2. EXPERIMENT

Of the five elements (Ni, Ge, Kr, Zr and Mo), studied in the present work, Ni is the most abundant high-Z impurity in the JET plasma. It has now been examined in a large number of plasma discharges under various conditions. The Kr spectra were recorded in connection with the work described in Ref. [1], and the results now reported originate from additional studies of those experimental data. The elements Ge, Zr and Mo were introduced into the plasma by means of the laser blow-off technique [15], but in some cases Mo also entered the plasma during neutral beam injection.

As the central electron temperatures for JET plasmas generally lie between 3 and 10 keV, B-like spectra of the elements mentioned above were obtained relatively easily. When Ge, Zr or Mo were injected into the plasma, the maximum central temperatures were between 5 and 9 keV.

As in the earlier work [1, 2] the spectra were recorded by means of a 2-m grazing incidence spectrometer [16], equipped with a 600 ℓ/mm grating and two microchannel-plate image intensifier-converter detector systems. The total detected spectral region extends from 20 to 335 Å with a wavelength resolution between 0.2 and 0.25 Å. The $n = 2$, $\Delta n = 0$ transitions, now studied, appeared in several diffraction orders. As reference lines we used transitions in C V and C VI, also in several orders, as well as lines in highly charged Ni [12]. Additional reference lines were taken from the recent papers by Feldman et al. [10, 11] and Sugar et al. [17].

The analysis of the spectra was carried out at the Lund University, using the deconvolution program CARATE [18] which fits the observed spectral lines to sums of Gaussians. Further details of the spectral analyses have been reported earlier [19, 20].

3. THEORETICAL CALCULATIONS

The well-known work of Cheng et al. [5] which based on the MCDF code of Desclaux [21], has been extensively used in many analyses of highly charged ions with 3 - 9 electrons, see e.g. Refs. [1-4]. It could also be used in the present work, despite the fact that for Z exceeding 30, data are given for selected values of Z only. However, as already stated, we also carried out new theoretical calculations - for B-like ions - using the MCDF code developed by Grant et al. [13, 14]. On the other hand, for F-like ions, where we only studied the fine-structure splitting of the ground state, we mainly used the theoretical data given by Huang et al. [22] and Kim and Huang [23] which represent improvements upon the earlier MCDF results [5], for the fine-structure separations of the ground term.

In the present MCDF calculations for B-like ions transitions between the ground configuration $1s^22s^22p$ and the lowest excited one, $1s^22s2p^2$, the odd configuration $1s^22p^3$, which interacts with the ground term, was included. Within the $n = 2$ complex there are no configurations that can interact with $1s^22s2p^2$ but here we investigated the interaction of $1s^22s2p^2$ with three $n = 3$ configurations, viz. $1s^22s3p^2$, $1s^22s^23d$ and $1s^22s3d^2$. The analyses showed that the interaction was most pronounced between $2s2p^2$ and $2s3d^2$, because of the $\left\langle 2p^2 | 1/r_{12} | 3d^2 \right\rangle$ pair correlation. Since our aim was to obtain reasonably good results with a limited basis set, only $1s^22s3d^2$, being the main perturber of $1s^22s2p^2$, was included. In the calculations the radial wavefunctions were optimised on the Extended Average Level (EAL) of the four configurations involved, whereas Breit corrections to the energy levels were included in the diagnolization of the Hamiltonian matrix (for details about this method, cf. [13] and [14]).

Cheng et al. [5] also calculated the Breit interation as well as Lamb shift contributions to the energy levels. However, Edlén [3, 4] noted that the calculated Lamb shift values did not exhibit a regular Z-dependence, and to overcome this he provided isoelectronically smoothed QED corrections. In the present work we have not calculated QED effects, partly because the difference between experimental and theoretical wavenumbers was found to be fairly small and regularly varying with Z even without including these corrections.

4. RESULTS AND DISCUSSION

4.1 Tokamak Observations

Two examples of JET spectra are depicted in Figs. 1 and 2. Of these Fig. 1 is part of a recording in first order, showing all our identified lines in the doublet system of B-like Mo XXXVIII. The three-dimensional Fig. 2 shows the temporal behaviour of the intensities for some transitions in highly charged Ge and Mo, following a simultaneous injection of these elements. In a number of cases the temporal variation of spectral line intensities was quite useful in assigning the ionization stages of the lines studied.

The lines identified in this work together with their estimated wavelength uncertainties are given in Table I. For F-like ions our new results are limited to observations of magnetic-dipole (M1) transitions within the ground term of Zr XXXII and Mo XXXIV. A similar M1 transition has now also been observed for B-like Mo XXXVIII, but for this sequence the majority of the new lines are due to electric-dipole (E1) transitions. Of the latter, the quartet-doublet intercombination lines were found for B-like Ni, Kr and Mo. In Table II we present the experimentally determined energy level values together with their uncertainties. The latter vary from 50 cm^{-1} to 1 500 cm^{-1}.

4.2 Theoretical Studies

Our calculated values for the transition energies in B-like ions will be given below, where we discuss and compare theoretical and experimental data in a more systematic way. A comparison of our theoretical results with those of

Cheng et al. [5], for one particular transition in B-like ions, $2s^22p\ ^2P_{1/2}$-$2s2p^2\ ^2D_{3/2}$, is shown in Fig. 3. (Similar trends were found for other transitions in B-like ions). For each value of the nuclear charge Z, the difference between theoretical and experimental transition energies is divided by (Z - 4). The data of Cheng et al., without or with Lamb shift (curves 1 and 2, respectively) are displayed, together with the results of our calculations, without or with inclusion of the $2s3d^2$ perturber (curves 3 and 4, respectively). It is interesting to note that the difference between the values of Cheng et al. [5] which include QED (curve 2) and experimental data is approximately linear, and that agreement with experiment is nearly perfect for Mo, Z = 42. Our results, being much closer to experiment than the values of Cheng et al. that do not include Lamb shifts (curve 1), exhibit a nearly constant deviation from the experimental data (Fig. 3). An interesting point is that a combination of our calculated data and the Lamb shifts given by Cheng et al. [5] results in larger differences from experimental data when Z increases. The reason for this is not clear, and further studies, including more elaborate theoretical analyses and experimental work (e.g. for Z > 42) are therefore motivated.

4.3 F-Like Ions

The lines classified as the $2s^22p^5(^2P_{3/2} - {}^2P_{1/2})$ magnetic dipole transitions in F-like Zr XXXII and Mo XXXIV are fairly prominent in our spectra which is expected for a high temperature, low density plasma such as in the JET tokamak. Because of the presence of only one reference line in its vicinity (the 3s $^2S_{1/2}$ - 3p $^2P_{3/2}$ transition in Zr XXX, at 142.839 Å [24]), the wavelength uncertainty of the Zr XXXII M1 line, at 140.15 Å, is somewhat larger than that quoted for most other transitions.

Theoretical and experimental data for the $2s^22p^5(^2P_{3/2} - {}^2P_{1/2})$ M1 transition in the F-like ions Cr XVI - Ag XXXIX are included in Table III. As the "best" theoretical data we used the values of Kim and Huang [23], which are compared with experimental results. The differences between theoretical and experimental wavenumbers vary smoothly with Z, and by fitting them to a second-degree polynomial we obtained recommended values of the fine-structure separations (in cm^{-1}) and wavelengths (in Å) of the M1 lines, see Table III. These results are in excellent agreement with similar data given in Refs. [4, 9, 11, 25]. For instance, our extrapolated wavelength of 68.51Å for Ag XXXIX is in accord with the values 68.48Å and 68.51Å, previously obtained by Reader et al. [9] and Feldman et al. [11], respectively. In this context, the semiempirical data of Curtis and Ramanujam [26], based on screening parametrization, should be mentioned. With new results now available, this method should be extended to higher values of Z.

4.4 B-Like Ions

In Table IV we list theoretical and experimental data for the $2s^22p$ ($^2P_{1/2}$ - $^2P_{3/2}$) M1 transition in the B-like ions V XIX - Mo XXVIII. As a source of theoretical data we have used the calculations of Huang et al. [22], which - as already stated - represented improvements on the results of Cheng et al. [5]. The fine-structure data of Huang et al. are also closer to the experimental results than our own theoretical values. By combining the data of Refs. [5] and [22] we obtained reliable interpolated values for ions not included in Ref. [22]. These results were then compared with experimentally determined fine-structure intervals, and it was thereby found that the small difference between theory and experiment can be approximated by a linear function of Z. The isoelectronically smoothed wavenumbers and wavelengths, obtained from this procedure, are collected in Table IV. It is worth noting that our wavelength of the Mo line, 103.696 Å (Table I), is quite close to extrapolated value, 103.71 Å, obtained by Edlén [3].

Tables I and II show that we have identified a number of transitions to the $2s^22p$ $^2P_{1/2,\,3/2}$ ground term from the $2s2p^2$ doublet levels, $^2S_{1/2}$, $^2P_{1/2,\,3/2}$ and $^2D_{3/2,\,5/2}$. Our calculations (as well as those of Cheng et al. [5]) predict large transition probabilities for the components $^2P_{1/2}$ - $^2D_{3/2}$, $^2P_{1/2}$ - $^2S_{1/2}$, $^2P_{3/2}$ - $^2P_{3/2}$, $^2P_{3/2}$ - $^2P_{1/2}$ and $^2P_{3/2}$ - $^2D_{5/2}$. For the first three in Mo XXXVIII our observed relative intensities are 1:0.8:0.1, and our data for Ge XXVIII and Kr XXXII are very similar. In a theoretical study of line intensities in tokamak plasmas, Feldman et al. [27] obtained the values of 1:1:0.09 and 1:0.85:0.04 for these ratios in B-like Ge and Kr, respectively. The agreement between experiment and theory is thus satisfactory.

Edlén [3] has pointed out the difficulties in analyzing the transitions from the $2s2p^2$ $^2S_{1/2}$ and $^2P_{1/2}$ levels to the ground term. The interaction between these excited levels has been studied theoretically by several authors, see e.g. [28 - 31], who have found that the levels exhibit an avoided crossing near Z = 22. It is customary to call the lower level $^2S_{1/2}$ and the higher $^2P_{1/2}$ throughout the sequence, although this means that "for the ions V^{+18} to Fe^{+21} the main contribution to $^2S_{1/2}$ is $^2P_{1/2}$ and vice versa" (Dankwort and Trefftz [30]). Tables V and VI present results for the $2s^22p$ $^2P_{1/2}$ - $2s2p^2$ $^2S_{1/2}$ and the $2s^22p$ $^2P_{3/2}$-

$2s2p^2\ ^2P_{1/2}$ combinations, respectively. The data for Ge, Kr and Mo, now obtained, fit well into the systematics and facilitate reliable interpolations to ions for which the experimental material is more fragmentary. It is interesting to compare the present results with the transition energies predicted by Edlén [3]. The latter do not go to higher ionization stages than B-like Kr, and represent extrapolated values for Z exceeding 28. In spite of this fact, the agreement between our data and Edlén's results is very satisfactory. In the case of Kr XXXII, the extrapolated transition energy [3] is 950 cm^{-1} (0.06%) too low for the $^2P_{1/2}$ - $^2S_{1/2}$ transition (Table V) and 1 020 cm^{-1} (0.07%) too high for the $^2P_{3/2}$ - $^2P_{1/2}$ combination (Table VI).

The results for transitions from the $2s2p^2\ ^2P_{3/2}$ and $^2D_{3/2}$ levels to the ground term are given in Tables VII and VIII. Being a comparatively weak line (see e.g. Fig. 1) the $^2P_{3/2}$ - $^2P_{3/2}$ combination has been observed for only three ions beyond Ni XXIV (Table VII), and this fact makes the fit somewhat uncertain. Additional experimental results exist for the more intense $^2P_{1/2}$ - $^2D_{3/2}$ line (Table VIII). In both cases the transition energies for Kr, extrapolated by Edlén [3], are somewhat higher than the data now obtained (using all available recent data), the differences being 1 420 cm^{-1} (0.09%) and 2 660 cm^{-1} (0.18%), respectively.

In Ni XXIV, Kr XXXII and Mo XXXVIII we have identified the $2s^22p\ ^2P_{1/2}$ - $2s2p^2$ $^4P_{1/2}$ and $^2P_{3/2}$ - $^4P_{5/2}$ intercombination lines. The intensities of such lines are known to be enhanced in low density plasmas such as the solar corona and tokamaks, but these transitions can also be studied by beam-foil spectroscopy, using the method of delayed spectra [32]. In the solar flare spectra, the intercombination multiplet ^2P - ^4P has been identified for B-like Fe XXII by Sandlin et al. [33]. The wavelength for the $^2P_{3/2}$ - $^4P_{5/2}$ transition for Ni XXIV has been predicted by Lawson and Peacock [34] to fall at 224.02 Å, whereas the analysis by Edlén [3] yielded 224.57 Å. In the present work we have found a line at 224.71 Å which is ascribed to the $^2P_{3/2}$ - $^4P_{5/2}$ transition. The $^2P_{1/2}$ - $^4P_{1/2}$ transition was found to be the strongest line of the ^2P-^4P multiplet, which is in accord with our calculations.

5. CONCLUSIONS

In the present work we have extended the observation of the n = 2 complex in B-like ions up to Mo XXXVIII by means of measurements at the JET tokamak. Among the classified lines are M1 transitions and spin-forbidden E1 transitions which are particularly valuable in plasma diagnostics. Using semi-empirical methods developed by Edlén we have extended the knowledge of B-like and F-like ions up to highly charged Mo. The spectra analysed in the present work also contain several new transitions in C-like and N-like ions, and these results will be published later.

ACKNOWLEDGEMENTS

Two of the authors (C.J. and R.M) are grateful to the JET management and team for the hospitality they enjoyed during their stay. The authors are indebted to Dr. J.O. Ekberg, Prof. H.P. Summers and a referee for their critical reading of the manuscript. The work has been supported by the Swedish Natural Science Research Council (NFR).

REFERENCES

[1] Denne, B., Hinnov, E., Ramette, J., and Saoutic,B., Phys. Rev. **A 40**, 1488 (1989).

[2] Denne, B., Magyar, G., and Jacquinot, J., Phys. Rev. **A 40**, 3702 (1989).

[3] Edlén, B., Physica Scripta **28**, 483 (1983).

[4] Edlén, B., Physica Scripta **28**, 51 (1983).

[5] Cheng, K.T., Kim, Y.-K. and Desclaux, J.P., Atomic Data and Nuclear Data Tables **24**, 111 (1979).

[6] Hinnov, E., Ramsey, A., Stratton, B., Cohen, S. and Timberlake, J., J. Opt. Soc. Am. **B 4**, 1293 (1987).

[7] Wouters, A., Schwob, J.L., Suckewer, S., Seely, J.F., Feldman, U., and Dave, J.H., Opt. Soc. Am. **B 5**, 1520 (1988).

[8] Feldman, U., Seely, J.F., Brown, C.M., Ekberg, J.O., Richardson, M.C., Behring, W.E. and Reader, J., J. Opt. Soc. Am. **B 3**, 1605 (1986).

[9] Reader, J., Brown, C.M., Ekberg, J.O., Feldman, U., Seely, J.F., and Behring, W.E., J. Opt. Soc. Am. **B 3**, 1609 (1986).

[10] Feldman, U., Ekberg, J.O., Brown, C.M., and Seely, J.F., J. Opt. Soc. Am. **B 6**, 1652 (1989).

[11] Feldman, U., Ekberg, J.O., Seely, J.F., Brown, C.M., Kania, D.R., MacGowan, B.J., Keane, C.J., and Behring, W.E., J. Opt. Soc. Am. **B 8**, 531 (1991).

[12] Sugar, J., Kaufman, V., and Rowan, W.L., J. Opt. Soc. Am. **B 9**, 344 (1992).

[13] Grant, I.P., McKenzie, B.J., Norrington, P.H., Mayers, D.F. and Pyper, N.C., Comp. Phys. Commun, **21**, 207 (1980).

[14] McKenzie, B.J., Grant, I.P., and Norrington, P.H., Comp. Phys. Commun. **21**, 233 (1980).

[15] Magyar, G., Barnes, M.R., Cohen, S., Edwards, A., Hawkes, N.C., Pasini, D. and Roberts, P.J., JET Report JET-R(88)15 (1988).

[16] Schwob, J.-L., Wouters A.W., Suckewer, S., and Finkenthal, M., Rev. Sci. Instr. **58**, 1601 (1987).

[17] Sugar, J., Kaufman, V., and Rowan, W.L., J. Opt. Soc. Am. **B 8**, 22 (1991), and references quoted therein.

[18] Carlén, L., Internal Report LUNFD 6/NFFK-7014), University of Lund (1982).

[19] Jupén, C., Denne, B., and Martinson, I., Physica Scripta **41**, 669 (1990).

[20] Jupén, C., Martinson, I., and Denne-Hinnov, B., Physica Scripta **44**, 562 (1991).

[21] Desclaux, J.P., Comp. Phys. Commun. **9**, 31 (1975).

[22] Huang, K.-N., Kim, Y.-K., Cheng, K.T., and Desclaux, J.P., Phys. Rev. Letters **48,** 1245 (1982).

[23] Kim, Y.-K., and Huang, K.-N., Phys. Rev. **A 26**, 1984 (1982).

[24] Reader, J., Kaufman, V., Sugar, J., Ekberg, J.O., Feldman, U., Brown, C.M., Seely, J.F. and Rowan, W.L., J. Opt. Soc. Am. **B 4**, 1821 (1987).

[25] Reader, J., Phys. Rev. **A 26**, 501 (1982).

[26] Curtis, L.J., and Ramanujam, P.S., Phys. Rev. **A 26**, 3672 (1982).

[27] Feldman, U., Seely, J.F., and Bhatia, A.K., Atomic Data Nucl. Data Tables **32**, 305 (1985).

[28] Sinanoglu, O., and Luken, W., J. Chem. Phys. **64**, 4197 (1976).

[29] Safronova, U.I. and Rudzikas, Z.B., J. Phys. **B 12**, 1989 (1976).

[30] Dankwort, W., and Trefftz, E., Astron. Astrophys. **65**, 93 (1978).

[31] Farrag, A., Luc-Koenig, E., and Sinzelle, J., At. Data Nucl. Data Tables **24**, 227 (1979).

[32] Träbert, E., Heckmann, P.H., Hutton, R., and Martinson, I., J. Opt. Soc. Am. **B 5**, 2173 (1988).

[33] Sandlin, G.D., Brueckner, G.E., Scherrer, V.E. and Tousey, R., Astrophys. J. **205**, L47 (1976).

[34] Lawson, K.D., and Peacock, N.J., J. Phys. **B 13**, 3313 (1980).

Table I. Classified Lines in F-Like and B-Like Ions

Ion	Transition	Wavelength (Å) This Work			Wavelength (Å) Previous Experiments
F I Sequence					
Zr XXXII	$2s^22p^5\,^2P_{3/2}$ - $2s^22p^5\,^2P_{1/2}$	140.150	±	0.040	
Mo XXXIV	$2s^22p^5\,^2P_{3/2}$ - $2s^22p^5\,^2P_{1/2}$	112.828	±	0.020	
B I Sequence					
Ni XXIV	$2s^22p\,^2P_{1/2}$ - $2s2p^2\,^4P_{3/2}$	185.283	±	0.030[a]	
	$2s^22p\,^2P_{1/2}$ - $2s2p^2\,^4P_{1/2}$	218.608	±	0.025	
	$2s^22p\,^2P_{3/2}$ - $2s2p^2\,^4P_{5/2}$	224.712	±	0.025	
Ge XXVIII	$2s^22p\,^2P_{1/2}$ - $2s2p^2\,^2S_{1/2}$	83.611	±	0.020	
	$2s^22p\,^2P_{1/2}$ - $2s2p^2\,^2D_{3/2}$	90.860	±	0.020	90.64[b]
	$2s^22p\,^2P_{3/2}$ - $2s2p^2\,^2P_{1/2}$	82.182	±	0.020	
Kr XXXII	$2s^22p\,^2P_{3/2}$ - $2s2p^2\,^2P_{3/2}$	64.651	±	0.010	64.65[c]
	$2s^22p\,^2P_{3/2}$ - $2s2p^2\,^2P_{1/2}$	65.067	±	0.025	
	$2s^22p\,^2P_{3/2}$ - $2s2p^2\,^2D_{5/2}$	84.454	±	0.025	84.94[c]
	$2s^22p\,^2P_{1/2}$ - $2s2p^2\,^4P_{1/2}$	143.266	±	0.010	
	$2s^22p\,^2P_{3/2}$ - $2s2p^2\,^4P_{5/2}$	151.121	±	0.025	
Mo XXXVIII	$2s^22p\,^2P_{3/2}$ - $2s2p^2\,^2P_{3/2}$	45.312	±	0.030	
	$2s^22p\,^2P_{3/2}$ - $2s2p^2\,^2P_{1/2}$	45.446	±	0.030	
	$2s^22p\,^2P_{1/2}$ - $2s2p^2\,^2S_{1/2}$	46.570	±	0.020	
	$2s^22p\,^2P_{1/2}$ - $2s2p^2\,^2D_{3/2}$	47.553	±	0.020	
	$2s^22p\,^2P_{1/2}$ - $2s2p^2\,^2P_{3/2}$	103.696	±	0.010	
	$2s^22p\,^2P_{1/2}$ - $2s2p^2\,^4P_{1/2}$	111.85	±	0.050[a]	
	$2s^22p\,^2P_{3/2}$ - $2s2p^2\,^4P_{5/2}$	121.098	±	0.025	

[a]Blended line [b]Wouters et al. [7], quoted uncertainty ± 0.01 Å
[c]Denne et al. [1], quoted uncertainty ± 0.10 Å

Table II. Energy Levels for F-Like and B-Like Ni, Ge, Kr, Zr and Mo

	Ion	Level	Energy Value (cm^{-1})
F-like	Zr XXXII	$2s^22p^5\ ^2P_{1/2}$	713 520 ± 200
	Mo XXXIV	$2s^22p^5\ ^2P_{1/2}$	886 305 ± 160
B-like	Ni XXIV	$2s2p^2\ ^4P_{1/2}$	457 440 ± 50
		$2s2p^2\ ^4P_{3/2}$	539 715 ± 90
		$2s2p^2\ ^4P_{5/2}$	608 975 ± 70
	Ge XXVIII	$2s2p^2\ ^2D_{3/2}$	1 100 600 ± 240
		$2s2p^2\ ^2S_{1/2}$	1 196 000 ± 280
		$2s2p^2\ ^2P_{1/2}$	1 511 320 ± 300
	Kr XXXII	$2s2p^2\ ^4P_{1/2}$	698 000 ± 50
		$2s2p^2\ ^4P_{5/2}$	1 154 280 ± 120
		$2s2p^2\ ^2D_{5/2}$	1 676 630 ± 350
		$2s2p^2\ ^2P_{1/2}$	2 029 440 ± 600
		$2s2p^2\ ^2P_{3/2}$	2 039 330 ± 250
	Mo XXXVIII	$2s2p^2\ ^4P_{1/2}$	894 050 ± 400
		$2s^22p\ ^2P_{3/2}$	964 050 ± 90
		$2s2p^2\ ^4P_{5/2}$	1 790 130 ± 200
		$2s2p^2\ ^2D_{3/2}$	2 102 900 ± 900
		$2s2p^2\ ^2S_{1/2}$	2 147 300 ± 900
		$2s2p^2\ ^2P_{1/2}$	3 164 770 ± 1500
		$2s2p^2\ ^2P_{3/2}$	3 171 300 ± 1500

Table III. The $2s2p^5(^2P_{3/2} - ^2P_{1/2})$ Transition in F-like Ions

Ion		σ_{th}[a] (cm^{-1})	σ_{exp} (cm^{-1})			σ_{fit} (cm^{-1})	λ_{fit} (Å)
Cr	XVI	70 919	70 892	±	5[b]	70 896	1 410.5
Mn	XVII	85 671	85 505	±	180[b]	85 637	1 167.7
Fe	XVIII	102 629	102 579	±	15[b]	102 581	974.84
Co	XIX	122 010	121 965	±	200[b]	121 954	820.04
Ni	XX	114 038	143 978	±	30[b]	143 954	694.67
Cu	XXI	168 953	168 833	±	50[b]	168 846	592.26
Zn	XXII	197 006	196 980	±	130[b]	196 874	507.94
Ga	XXIII	228 457	228 379	±	140[b]	228 297	438.03
Ge	XXIV	263 583	263 435	±	70[b]	263 391	379.66
As	XXV	302 671	302 678	±	200[b]	302 445	330.64
Se	XXVI	346 022	345 901	±	60[c]	345 759	289.22
Br	XXVII	393 949				393 646	254.04
Kr	XXVIII	446 783	446 438	±	60[d]	446 438	224.00
Rb	XXIX	504 863				504 472	198.23
Sr	XXX	568 547	568 360	±	400[b]	568 107	176.02
Y	XXXI	638 207	637 270	±	500[b]	637 716	156.81
Zr	XXXII	714 231	713 521	±	200[e]	713 685	140.12
Nb	XXXII	797 023				796 420	125.56
Mo	XXXIV	887 003	886 305	±	160[e]	886 340	112.82
Tc	XXXV	984 608				983 882	101.64
Ru	XXXVI	1 090 292				1 089 500	91.79
Rh	XXXVII	1 204 529				1 203 668	83.08
Pd	XXXVIII	1 327 816				1 326 883	75.37
Ag	XXXIX	1 460 655				1 459 648	68.51

[a]Kim and Huang [23]

[b]Edlén [4]

[c]Hinnov et al. [6]

[d]Denne et al. [1]

[e]This work

Table IV. The $2s^22p^5(^2P_{1/2} - ^2P_{3/2})$ Transition in B-like Ions

Ion		σ_{th}[a] (cm^{-1})	σ_{exp} (cm^{-1})	σ_{fit} (cm^{-1})	λ_{fit} (Å)
V	XIX	68 547	68 606 ± 40[b]	68 635	1 457.0
Cr	XX	82 858	82 926 ± 20[b]	82 939	1 205.7
Mn	XXI	99 330	99 287 ± 110[b]	99 404	1 006.0
Fe	XXII	118 173	118 266 ± 20[b]	118 240	845.74
Co	XXIII	139 614		139 674	715.95
Ni	XXIV	163 888	163 961 ± 50[b]	163 941	609.98
Cu	XXV	191 246	191 278 ± 70[b]	191 292	522.76
Zn	XXVI	221 945		221 984	450.48
Ga	XXVII	256 262		256 294	390.18
Ge	XXVIII	294 481		294 506	339.55
As	XXIX	336 906		336 924	296.80
Se	XXX	383 845	383 833 ± 75[c]	383 857	260.51
Br	XXXI	435 628		435 633	229.55
Kr	XXXII	492 599	492 560 ± 50[d]	492 597	203.01
Rb	XXXIII	555 108		555 099	180.15
Sr	XXXIV	623 535		623 519	160.38
Y	XXXV	698 259		698 236	143.22
Zr	XXXVI	779 687		779 657	128.26
Nb	XXXVII	868 249		868 212	115.18
Mo	XXXVIII	964 344	964 357 ± 100[e]	964 300	103.70

[a]Huang et al. [22]
[b]Edlén [3]
[c]Hinnov et al. [6]
[d]Denne et al. [1]
[e]Present Work

Table V. The $2s^22p\ ^2P_{1/2}$ - $2s2p^2\ ^2S_{1/2}$ Transition in B-like Ions

Ion		σ_{th} [a] (cm^{-1})	σ_{exp} (cm^{-1})	σ_{fit} (cm^{-1})	λ_{fit} (Å)
V	XIX	724 795	716 384 ± 100[b]	716 303	139.61
Cr	XX	769 468	760 341 ± 115[b]	760 338	131.52
Mn	XXI	815 721	805 997 ± 130[b]	806 042	124.06
Fe	XXII	863 797	853 388 ± 110[b]	853 652	117.14
Co	XXIII	913 985		903 252	110.69
Ni	XXIV	966 576	955 758 ± 45[c]	955 726	104.63
Cu	XXV	1 021 878		1 010 779	98.934
Zn	XXVI	1 080 216	1 068 147 ± 230[d]	1 068 930	93.551
Ga	XXVII	1 141 956		1 130 538	88.453
Ge	XXVIII	1 207 437	1 196 014 ± 280[a]	1 195 939	83.616
As	XXIX	1 277 057		1 265 523	79.019
Se	XXX	1 351 205	1 339 405 ± 900[e]	1 339 675	74.645
Br	XXXI	1 430 267	1 418 800 ± 200[f]	1 418 776	70.483
Kr	XXXII	1 514 669	1 502 900 ± 570[g]	1 503 245	66.523
Rb	XXXIII	1 604 827		1 593 494	62.755
Sr	XXXIV	1 701 172		1 689 948	59.173
Y	XXXV	1 804 142		1 793 039	55.771
Zr	XXXVI	1 914 205		1 903 231	52.542
Nb	XXXVII	2 031 777		2 020 933	49.482
Mo	XXXVIII	2 157 904	2 147 305 ± 900[a]	2 147 187	46.573

[a]This Work
[b]Edlén [3]
[c]Sugar et al. [12]
[d]Wouters et al. [7]
[e]Hinnov et al. [6]
[f]Feldman et al. [10]
[g]Denne et al. [1]

Table VI. The $2s^22p\ ^2P_{3/2}$ - $2s2p^2\ ^2P_{1/2}$ Transition in B-like Ions

Ion		σ_{th}^{a} (cm^{-1})	σ_{exp} (cm^{-1})	σ_{fit} (cm^{-1})	λ_{fit} (Å)
V	XIX	730 066	720 218 ± 110[b]	720 110	138.89
Cr	XX	773 922	764 811 ± 120[b]	764 602	130.79
Mn	XXI	819 954	811 455 ± 130[b]	811 187	123.28
Fe	XXII	868 372	859 946 ± 120[b]	860 087	116.27
Co	XXIII	919 397	911 584 ± 150[b]	911 532	109.71
Ni	XXIV	973 274	965 754 ± 50[c]	965 777	103.54
Cu	XXV	1 030 269		1 023 099	97.742
Zn	XXVI	1 090 643		1 083 767	92.271
Ga	XXVII	1 154 707		1 148 102	87.100
Ge	XXVIII	1 222 777		1 216 430	82.208
As	XXIX	1 295 169		1 289 078	77.575
Se	XXX	1 372 231		1 366 402	73.185
Br	XXXI	1 454 333	1 448 792 ± 510[d]	1 448 783	69.023
Kr	XXXII	1 541 829	1 536 877 ± 500[e]	1 536 585	65.079
Rb	XXXIII	1 635 135		1 630 233	61.341
Sr	XXXIV	1 734 605		1 730 090	57.800
Y	XXXV	1 840 705		1 836 634	54.447
Zr	XXXVI	1 953 811		1 950 249	51.276
Nb	XXXVII	2 074 430		2 071 312	48.275
Mo	XXXVIII	2 202 934	2 200 413 ± 1500[a]	2 200 626	45.442

[a]This Work
[b]Edlén [3]
[c]Sugar et al. [12]
[d]Feldman et al. [10]
[e]Denne et al. [1]

Table VII. The $2s^22p\ ^2P_{3/2}$ - $2s2p^2\ ^2P_{3/2}$ Transition in B -Like Ions

Ion		σ_{th}^{a} (cm^{-1})	σ_{exp} (cm^{-1})	σ_{fit} (cm^{-1})	λ_{fit} (Å)
V	XIX	749 766	733 933 ± 130[b]	733 858	136.27
Cr	XX	794 458	778 670 ± 150[b]	778 558	128.448
Mn	XXI	841 064	825 272 ± 170[b]	825 247	121.18
Fe	XXII	889 822	874 040 ± 150[b]	874 070	114.41
Co	XXIII	941 008	925 680 ± 220[b]	925 332	108.07
Ni	XXIV	994 896	979 288 ± 50[c]	979 306	102.11
Cu	XXV	1 051 779		1 036 282	96.499
Zn	XXVI	1 111 976		1 096 578	91.193
Ga	XXVII	1 175 806		1 160 512	86.169
Ge	XXVIII	1 243 596		1 228 407	81.406
As	XXIX	1 315 702		1 300 619	76.886
Se	XXX	1 392 486		1 377 508	72.595
Br	XXXI	1 474 295	1 459 449 ± 500[d]	1 459 420	68.520
Kr	XXXII	1 561 548	1 546 766 ± 250[e]	1 546 770	64.651
Rb	XXXIII	1 654 588		1 639 902	60.979
Sr	XXXIV	1 753 832		1 739 229	57.497
Y	XXXV	1 859 738		1 845 209	54.194
Zr	XXXVI	1 972 658		1 958 191	51.068
Nb	XXXVII	2 091 311		2 076 892	48.149
Mo	XXXVIII	2 221 432	2 206 920 ± 1500[a]	2 207 048	45.309

[a]This Work
[b]Edlén [3]
[c]Sugar et al. [12]
[d]Feldman et al. [10]
[e]Denne et al. [1]

Table VIII. The $2s^22p\ ^2P_{1/2}$ - $2s2p^2\ ^2D_{3/2}$ Transition in B-Like Ions

Ion		σ_{th} [a] (cm^{-1})	σ_{exp} (cm^{-1})	σ_{fit} (cm^{-1})	λ_{fit} (Å)
V	XIX	601 887	597 291 ± 70[b]	597 261	167.43
Cr	XX	645 686	640 932 ± 80[b]	641 005	156.01
Mn	XXI	692 056	687 511 ± 100[b]	687 300	145.50
Fe	XXII	741 191	736 544 ± 110[b]	736 350	135.81
Co	XXIII	793 298	788 897 ± 125[b]	788 361	126.85
Ni	XXIV	848 594	843 505 ± 35[c]	843 551	118.55
Cu	XXV	907 301		902 143	110.85
Zn	XXVI	969 659	964 320 ± 150[d]	964 374	103.69
Ga	XXVII	1 035 925		1 030 504	97.040
Ge	XXVIII	1 106 366	1 100 594 ± 240[a]	1 100 798	90.843
As	XXIX	1 181 251		1 175 527	85.068
Se	XXX	1 260 890	1 255 178 ± 790[e]	1 254 999	79.681
Br	XXXI	1 345 587	1 339 700 ± 500[f]	1 339 518	74.654
Kr	XXXII	1 435 709	1 429 450 ± 410[g]	1 429 453	69.957
Rb	XXXIII	1 531 581		1 525 127	65.568
Sr	XXXIV	1 633 586		1 626 924	61.466
Y	XXXV	1 742 129		1 735 249	57.629
Zr	XXXVI	1 857 596		1 850 488	54.040
Nb	XXXVII	1 980 394		1 973 047	50.683
Mo	XXXVIII	2 111 085	2 102 916 ± 900[a]	2 103 490	47.540

[a]This Work
[b]Edlén [3]
[c]Sugar et al. [12]
[d]Wouters et al. [12]
[e]Hinnov et al. [6]
[f]Feldman et al. [10]
[g]Denne et al. [1]

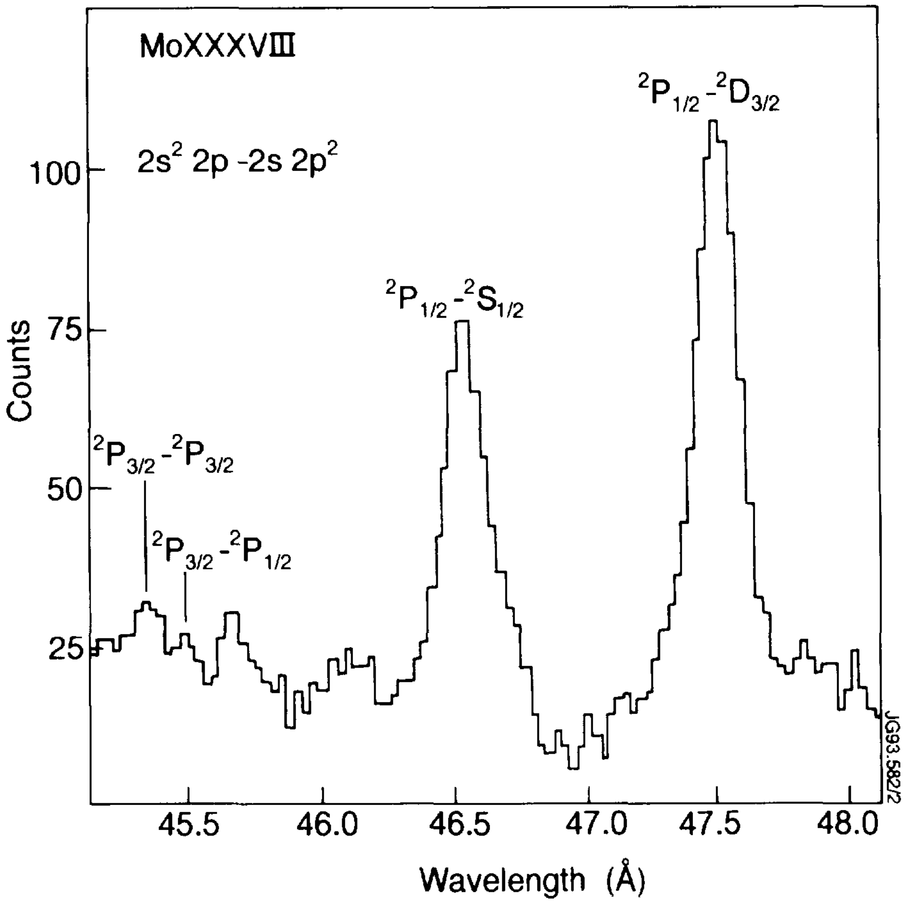

Fig. 1: Part of a JET spectrum, showing four of the $2s^22p$ - $2s2p^2$ transitions in B-like Mo XXXVIII.

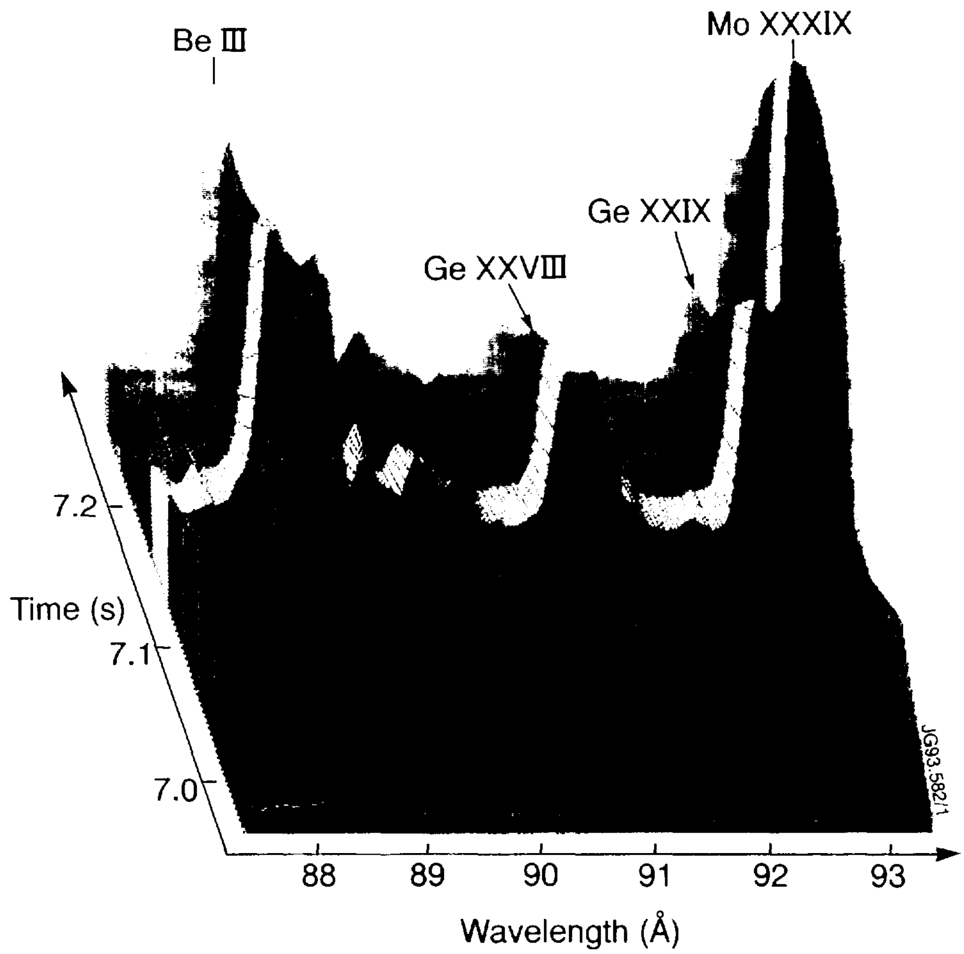

Fig. 2: A three dimensional recording from JET, showing transition in Be and highly ionized Ge and Mo.

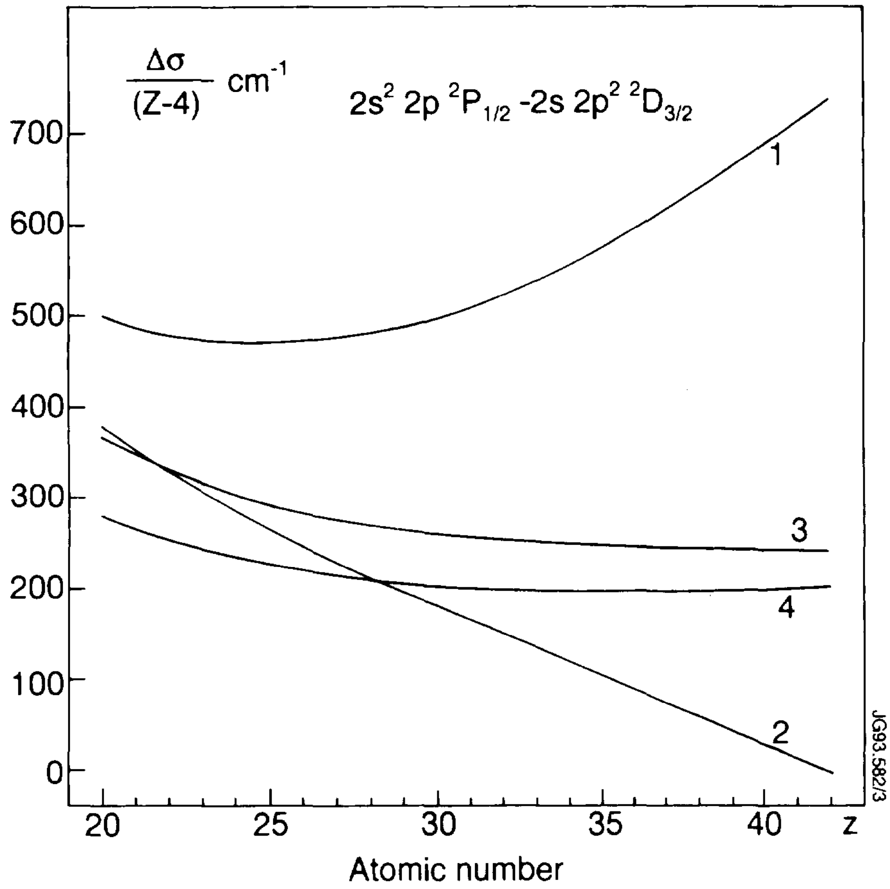

Fig. 3: Scaled differences between theoretical and experimental wavenumbers for the $2s^22p\ ^2P_{1/2}$ - $2s2p^2\ ^2D_{3/2}$ transition in the B-like ions Ca XXVI - Mo XXXVIII. The curves (1) and (2) are based on the work of Cheng et al. [5], with Lamb shift omitted (1) or included (2). Curves (3) and (4) show the differences between the present calculations and experiment, the $2s3d^2$ configuration being included in the case of curve (4) - see text.